0254-6124/2012/32(5)-665–16 *Chin. J. Space Sci.* 空间科学学报

Liu Libo, Wan Weixing, Chen Yiding, Le Huijun, Zhao Biqiang. Recent progresses on ionospheric climatology investigations. *Chin. J. Space Sci.*, 2012, **32**(5): 665-680

Recent Progresses on Ionospheric Climatology Investigations

LIU Libo WAN Weixing CHEN Yiding LE Huijun ZHAO Biqiang

(*Beijing National Observatory of Space Environment, Institute of Geology and Geophysics, Chinese Academy of Sciences, Beijing* 100029)

Abstract The ionosphere varies over multiple time scales, which are classified into two categories: the climatology and weather variations. In this national report, we give a brief summary of recent progresses in ionospheric climatology with focus on (1) the seasonal variations, (2) solar cycle effects, and (3) empirical modeling of the ionosphere. The seasonal variations of the ionosphere have been explored in many works to give a more detailed picture with regional and global features at various altitudes by analyzing the observation data from various sources and models. Moreover, a series of studies reported the response of the ionosphere to solar cycle variations, which revealed some novel and detailed features of solar activity dependence of ionospheric parameters at different altitudes. These investigations have improved our understanding on the states of the ionosphere and underlying fundamental processes, provided clues to future studies on ionospheric weather, and guided ionospheric modeling, forecasting and related applications.

Key words Ionosphere, Climatological variation, Seasonal variations, Solar cycle, Ionospheric modeling

Classified index P 353

1 Introduction

The ionosphere is formed under the ionization effect of solar X-ray and Extreme Ultraviolet (EUV) radiation. At the same time, the ionosphere is buffeted by sources from solar winds and magnetospheric activities. The lower atmospheres also contribute considerably to the variability of the ionosphere. As a consequence, a variety of periodic and aperiodic variations are observed in the ionosphere, with time scales ranging from the order of the solar cycle (11-year) to just a few seconds. In this national report to COSPAR, the ionospheric climatology is termed the averaged behaviors of the ionosphere with time coverage longer than the solar rotation period.

With the development of sounding techniques, the spatial coverage of ionospheric observations has got much better. Moreover, several global data centers have been established and opened for access, which ensure the data easily available for researchers. All of the above conditions make it possible for huge progress in ionosphere researches, particularly in climatology.

The seasonal variation, solar activity modulation, and long term trend of the ionosphere are fundamental problems of the ionospheric climatology. The

Received April 17, 2012

E-mail: liul@mail.igcas.ac.cn

studies on those issues are helpful for understanding ionospheric chemical and dynamical processes and have critical applications for empirical ionospheric modeling as well.

In this report, we give a brief introduction to the progresses of ionospheric climatology in recent several years. Our interest is mainly on (1) the seasonal variations, (2) solar cycle effects, and (3) empirical models of the ionosphere. The seasonal variations of the ionosphere have been explored to give a detailed picture with regional and global features at various altitudes by analyzing the observation data from various sources and models. Moreover, a series of works reported the response of the ionosphere to solar cycle variations, revealing novel and detailed features of solar activity dependence of ionospheric parameters at varying altitudes. These investigations have improved our understanding on the states of the ionosphere and underlying fundamental processes, provided clues to future studies on ionospheric weather, and guided ionospheric modeling, forecasting and related applications.

2 Seasonal Variation

The seasonal variation of the ionosphere is a traditional issue in ionospheric physics. It has been studied for decades, but there remain many unresolved problems. Chapman's ionization theory is usually used to predict the behaviors of the ionosphere. Sometimes, however, the peak density of F_2-layer ionosphere (N_mF_2) actually changes in a way inconsistent with the prediction of Chapman's ionization theory. Anomalies are taken to term the ionosphere under such situations with features significantly away from the theory's predictions. There are some anomalies in seasonal variations[1]. The principal anomalies observed include winter or seasonal anomaly (greater daytime N_mF_2 in winter than in summer), semiannual anomaly (higher N_mF_2 in equinoxes than in solstices), and annual anomaly or December anomaly (higher N_mF_2 in December than in June).

To show the seasonal feature of the ionosphere, ionospheric key parameters are often analyzed to obtain the principal components with periods no longer than a year. Yu *et al.*[2] collected the critical frequency of F_2-layer (f_0F_2) recorded at global 104 stations to reveal the latitudinal dependence of annual and semiannual components of daytime N_mF_2 for solar maxima. Their results show the following. (1) The annual component of N_mF_2 in both hemispheres dominates in the regions from 40° to 60° magnetic latitudes and becomes less significant at lower latitudes. Winter anomaly usually manifests strongly at higher latitudes and becomes less obvious or disappears at lower latitudes. (2) The semi-annual variations with peaks in equinox are generally weak in the near-pole regions and strong in the far-pole regions of both hemispheres. (3) In tropical regions the semiannual components are more significant than the annual components.

Yu *et al.* [3] gave a global distribution of the annual and semiannual components of Total Electron Content (TEC) in 2000 (a year at solar maximum) through retrieving the TEC data from the international Global Positioning System (GPS) service center (IGS). Their results show that the annual amplitudes of daytime TEC have larger values at middle and high latitudes in both hemispheres and smaller in equatorial and low latitude regions. In contrast, the semiannual amplitudes are larger in far-pole regions than in near-pole regions. Moreover, in most regions the peak TEC appears in equinoctial months, while the maximum values appear in winter in northern near-pole regions and in summer in South America and Australian. Similar to N_mF_2, the seasonal variation of TEC is mainly attributed to the combined effects of changes in atmospheric composition $[O]/[N_2]$ and the photo-ionization production rates controlled by solar zenith.

Through introducing the Empirical Orthogonal Function (EOF) analysis, Zhao *et al.*[4] determined the EOF spatial base functions and temporal base functions in daily evolution of global distribution of

the Jet Propulsion Laboratory (JPL) Global Ionospheric Maps (GIMs) of TEC during the period from 1999 to 2005 and further presented the seasonal variation of TEC. The EOF spatial bases revealed significant seasonal anomaly in the time interval of 10:00 LT−15:00 LT at middle latitudes and semiannual anomaly in equatorial ionization anomaly region being strongest near 20:00 LT and weakest around sunrise. The EOF temporal bases indicate strong solar cycle effects on the seasonal variations of TEC. The contributions of seasonal anomaly and annual anomaly to the variability of TEC are larger than those of semiannual variations. They also found prominent equinoctial asymmetries in East Asia and South Australian regions. Further analysis of TIMED GUVI columnar $[O]/[N_2]$ data shows that the $[O]/[N_2]$ variation is a major contributor to the daytime winter anomaly of TEC.

Liu *et al.*[5] collected the JPL GIMs to detect the overall climatology of TEC during 1998−2008 in a new way. They evaluated the mean TEC which were averaged over the globe, and over low, middle and high latitude bands, respectively. These mean TECs present that the annual and semiannual components are dominant in seasonal variations. The annual asymmetry between June and December can be detected easily in the global and low latitude mean TEC for all solar activities and in middle latitude and high latitude mean TEC under most solar activities. The annual variations of the mean TEC are more significant in the southern hemisphere, while the semiannual variations are in phase and have comparable amplitudes in both hemispheres. The inter-hemispheric asymmetry of the mean TEC averaged in one hemisphere follows the variation of solar declination. Both the inter-hemispheric and annual asymmetries become stronger with increasing solar activity. Afraimovich *et al.*[6] and She *et al.*[7] also conducted an evaluation of mean TEC, which were averaged over the globe. However, when we try to adopt the mean TEC for indicating the variability of the ionosphere, these TECs averaged over the globe and in both hemispheres as well should be used with caution. It may provide false information on the ionosphere, especial under low solar activity. Under some situations the ionosphere actually dominates with annual variations, while the mean TEC averaged over both hemispheres definitely show significant semiannual variations.

Zhao *et al.*[8] applied an EOF analysis to examine the climatology of the topside ionosphere. The data used are the total ion density N_i at 840 km altitude, observed by the Scintillation Meter onboard the Defense Meteorological Satellite Program (DMSP) spacecraft in two Local Time (09:30 LT and 21:30 LT) sectors during the period of 1996−2004. The first EOF mode of the N_i variability is modulated by the intensity of solar EUV flux. The second EOF presents an annual asymmetry. The semiannual variation appears in the third EOF mode for the evening sector. The N_i variability is rapidly convergent; therefore it is very convenient to adopt the EOF expansion to construct an empirical model. The prediction accuracy of the model depends mainly on the first few principal components.

Liu *et al.*[9] further presented some salient features in the 10-year (1996−2005) topside plasma density recorded by the DMSP in the magnetic latitude range of 60°S−60°N. Strong yearly variations are shown in the longitude-average topside plasma density. In particular, annual components are predominant at most latitudes with maxima around the June solstice in the Northern Hemisphere and the December solstice in the Southern Hemisphere. Seasonal anomaly only occurs in the northern equatorial regions. Moreover, the differences of plasma densities between the two solstices are not symmetrical about the magnetic equator, being generally higher in the Southern Hemisphere than in the Northern Hemisphere. Conjugate-average plasma density is substantially greater at the December solstice than at the June solstice, which is modulated by solar activity levels and has latitudinal and longitudinal structures. The longitude effects of the annual asymmetry

depend on local time, being stronger in the evening sector than in the morning sector.

Accumulated evidence indicates that the winter anomaly only occurs in a limited altitude range in the ionosphere. What we do not know is where the winter anomaly will disappear. Clues may be inferred from synthetical analysis of the observations from ROCSAT (at about 600 km altitude), DMSP (840 km) and DEMETER (710 km) [10] satellites and those from COSMIC radio occultations as well.

COSMIC (a Constellation Observing System for Meteorology, Ionosphere and Climate mission of six microsatellites) was successfully launched to 512 km altitude in April 2006. The six satellites initially were close to each other, then they moved gradually to orbits at around 800 km altitudes. The COSMIC radio occultation observations have accumulated more than 2 000 000 electron density (N_e) profiles, providing us an excellent 3-D monitoring of the ionosphere. Liu *et al.*[11] collected the COSMIC measurements to investigate the seasonal behaviors of daytime N_e in the altitude range from 200 to 560 km. Harmonic analysis of N_e at different altitudes provides unprecedented details of the seasonal behaviors of N_e at Low Solar Activity (LSA).

Fig. 1, taken from Fig. 1 of Liu *et al.*[11], shows maps of A_{12} (the annual amplitude), A_6 (the semiannual amplitude), Φ_{12} (the annual phase), Φ_6 (the semiannual phase), A_0 (annual mean), A_{12}/A_0, A_6/A_0 and A_{12}/A_6 of the COSMIC N_e at altitudes of 204, 250, 340 and 500 km at 13:00 LT. In each panel the white curve indicates the dip equator, and two magenta circles represent the locations of magnetic poles. A_{12}, A_6 and A_0 are in units of $10^5\,\mathrm{cm}^{-3}$, and Φ_{12} and Φ_6 are in months.

Fig. 1 indicates that even during solar minimum there are strong and complicated annual and semiannual variations in daytime N_e, which have distinct latitudinal and altitudinal dependencies. The semiannual component predominates over the annual variation in equatorial regions and at high latitudes in the East Asian and South Atlantic sectors at low altitudes, and at higher altitudes the semiannual component predominates in equatorial region but recedes in other regions. The semiannual variation peaks in equinoctial months in most regions, while it has maxima in solstice months firstly in the South Pacific region (around 30° S, 120° W) at 250 km altitude then expanding over the South Pacific and South Atlantic Ocean at higher altitudes. Moreover, there is a region (around 45° S, 30° W) with dominant semiannual component, moving in the east-north direction with increasing altitude in the altitude range from 200 to 270 km. The relative amplitude of the N_e annual component has hemispheric asymmetry, which is prominent at high altitudes in the southern hemisphere. The winter/seasonal anomaly widely exists in the northern hemisphere and southern low latitudes and in Indian Ocean region at low altitudes but gradually disappears at higher altitudes.

Furthermore, in equatorial regions, a new finding is the obvious wave-like pattern in the longitudinal structure of the amplitudes of seasonal harmonic components in equatorial regions, which supports possible couplings between lower atmospheric origins and the longitudinal variations of N_e. Liu *et al.*[11] further illustrated the longitudinal structures of the key parameters of the F_2 peak (peak density and height and Chapman scale height) derived from the COSMIC data.

The results presented by Liu *et al.*[11] indicated that the phase of the annual variation of h_mF_2 is closely related to the sign of geomagnetic dip angle. The annual component of h_mF_2 definitely predominates in most regions, and the semiannual amplitude of h_mF_2 is particularly weaker. Zhang *et al.*[12] also gave a picture of the seasonal variations of ionospheric profiles at high and middle latitudes, in terms of the measurements of incoherent scatter radars during the International Polar Year (IPY).

The equinoctial asymmetry is an interesting and open question in ionospheric seasonal variations. Ho-

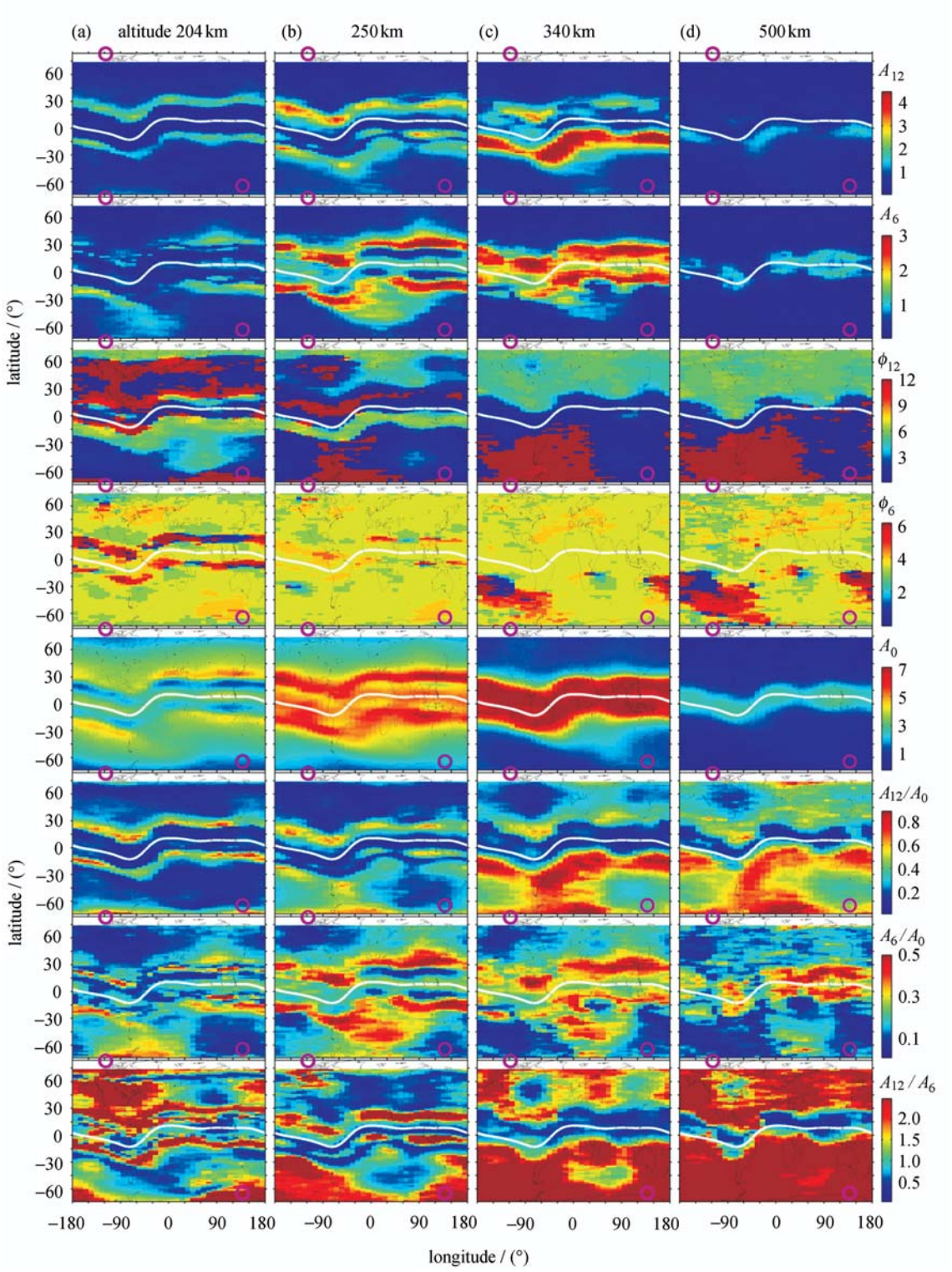

Fig. 1 Maps of A_{12} (the amplitude of the annual component), A_6 (the amplitude of the semiannual component), Φ_{12} (the phase of the annual component), Φ_6 (the phase of the semiannual component), A_0 (annual mean), A_{12}/A_0, A_6/A_0, and A_{12}/A_6 of the COSMIC N_e at 13:00 LT. In each panel the white curve indicates the dip equator, and two magenta circles represent the locations of magnetic poles. A_{12}, A_6 and A_0 are in units of $10^5\,\mathrm{cm}^{-3}$, Φ_{12} and Φ_6 are in months. After Liu *et al.*[11]

wever, it has not received enough attention in past investigations. For example, almost all ionospheric empirical models cannot reproduce the differences between March Equinox and September Equinox. In other words, these models did not treat the data in the two equinoxes separately. In the literature, there is not much information about the global picture for the equinoctial asymmetry. Balan *et al.*[13] collected the historical data observed from the Japanese MU incoherent scatter radar and showed higher electron densities in September equinox than in vernal months at lower altitudes. In contrast, the pattern is reversed at altitudes around and above the F_2 peak. They put forward that the equinoctial asymmetry in neutral wind should be responsible for the observed pattern in the topside ionosphere.

Liu *et al.*[14] utilized multiply ionospheric data, including global measurements of N_e profiles from COSMIC mission radio occultation measurements, ionosonde N_mF_2, TEC from TOPEX and Jason-1 and from global dual-frequency GPS receivers as well, to investigate the behaviors of the daytime ionosphere around equinoxes during Low Solar Activity (LSA). The analysis reveals that during LSA the equinoctial asymmetry in ionospheric plasma density is mainly a low latitude phenomenon. The equinoctial differences in TEC and N_mF_2 are remarkable at low latitudes in both hemispheres and less significant at higher latitudes. At higher altitudes, the asymmetry in COSMIC N_e becomes less significant in the southern hemisphere, and the pronounced asymmetry regions in the northern hemisphere move toward the magnetic equator. However, Chen *et al.*[15] recently revealed that the latitudinal features of the equinoctial asymmetry of N_mF_2 and TEC at high solar activity are different from those at low solar activity. At high solar activity, the equinoctial asymmetry of N_mF_2 is more prominent at middle latitudes while the equinoctial asymmetry of TEC is significant at all latitudes. In fact, the ionospheric equinoctial asymmetry should be considered as a manifestation of the annual variation, whose annual phase significantly shifts away from the solstices. According to this investigation, future models should treat the ionosphere on the two equinoxes separately, at least in the low latitude regions.

The F_2-layer peak height (h_mF_2) estimated from the COSMIC N_e profiles also shows an equinoctial asymmetry at low latitudes, indicating the existence of equinoctial differences in low latitude neutral winds, specifically in the northern hemisphere. However, the pattern of equinoctial asymmetry in h_mF_2 does not support the explanation of the absolute role of neutral wind effect on that of N_mF_2 as proposed by Balan *et al*[13]. Therefore, besides the important effect of the neutral wind, there should be other physical processes playing key roles in forming the observed equinoctial asymmetry in the ionosphere.

Ren *et al.*[16] investigated the equinoctial asymmetry in the vertical plasma drift velocity in equatorial F regions based on the ROCSAT-1 observations during the period from 1999 to 2004. The ROCSAT-1 ionospheric observations exhibit noticeable asymmetry in plasma drifts with obvious local time dependency. On the basis of the plasma drift observations, they also simulated the effect of the equinoctial asymmetry in plasma drift on ionospheric plasma density with the Theoretical Ionospheric Model of the Earth, Institute of Geology and Geophysics, Chinese Academy of Sciences (TIME-IGGCAS). The simulations indicate that the daytime equinoctial asymmetry in plasma drift could partly explain that in plasma density observed by Liu *et al*[14].

Currently, the atmospheric circulation mechanism is a widely accepted hypothesis for the ionospheric seasonal variations[1]. Solar radiation and Joule heating in the polar region are the main heating sources for the upper atmosphere. The input energy controls the convection pattern of the atmospheric circulation, changes the atmospheric composition, and further modulates the seasonal variation of the ionosphere. A simplified sketch is the summer-to-winter flow, which is driven by solar heating. In the summer hemisphere rich-N_2 is carried upwelling with the heated air, and downwelling occurs in the winter

hemisphere; as a result, the $[O]/[N_2]$ ratio decreases in the summer hemisphere and increases in the winter hemisphere. On the other hand, the summer-to-winter flow is reinforced by the effect of the summer auroral oval. Joule heating in the winter hemisphere also drives a subsidiary circulation[1].

Fuller-Rowell *et al.*[17] proposed the effect of "thermospheric spoon" to explain the semiannual variation, which is significant in the thermosphere. According to their theory, the cross-hemispheric general circulation acts as a spoon in the summer hemisphere to better mix the thermospheric compositions, compared to equinoctial months. The consequence is that the thermosphere as a whole is more molecular (*i.e.*, lower $[O]/[N_2]$) at solstice than at equinox. This also explains the F_2-layer semiannual effect in N_mF_2 prevailing at low and middle latitudes.

Oliver *et al.*[18] discussed the physical causes of middle latitude F layer behaviors. They emphasized the effect of neutral winds on h_mF_2 and the composition control of N_mF_2. Ma *et al.*[19−20] studied the semiannual variations in low-latitude f_0F_2 and in equatorial electrojet and proposed that the lower thermospheric diurnal tides modulate the semiannual variation of equatorial electric fields, which causes the semiannual variation in the low latitude ionosphere. Yu *et al.*[21] conducted simulations to examine the control of electric fields on N_mF_2 under solar minimum and geomagnetic quiet conditions. Their results indicate that the semiannual variation of electric field would strengthen that of N_mF_2 over equatorial anomaly regions in the afternoon to early morning hours.

Another open question is the annual asymmetry in F_2 layer. Although this feature has been detected for decades, its principal causes are not fully understood. Zeng *et al.*[22] investigated global variations of the annual asymmetry observed from 1-year COSMIC ionospheric radio occultation measurements. The COSMIC observations reveal strong annual asymmetry in N_mF_2 with significant longitudinal and local time variations. The numerical simulations using the Thermosphere-Ionosphere Electrodynamics Global Circulation Model (TIEGCM) are in very good agreement with the COSMIC observations. TIEGCM simulations indicate that differences in solar EUV radiation between the December and June solstices (due to the change in the Sun-Earth distance) and the displacement of the geomagnetic axis from the geographic axis are the two primary processes that cause the annual asymmetry and its associated longitudinal and local time variations. Although Zeng *et al.*[22] declared that the tides originating from lower atmosphere only have a minor contribution to this asymmetry, its quantitative contribution is not clear up to now.

Accumulated evidence indicates the tides originating from the lower atmosphere closely control the temporal and spatial structure of the ionosphere[23]. For example, the longitudinal ionospheric structure of wave number 4 may be linked with the atmospheric tide of nonmigrating tidal mode DE3 (diurnal eastward wave number 3). It is surely a challenge topic on the contributions of tides to the detailed structure of seasonal variations in the ionosphere.

Using ionosonde data from 33 stations in three longitude sectors from 1969 to 1986, Xu *et al.*[24] detected a periodic oscillation in daytime N_mF_2 with a period of 4 months (terannual), which is stronger in the midlatitude region in the Northern Hemisphere than in the Southern Hemisphere. In contrast, the terannual oscillation signature is not obvious in the nighttime F_2 layer. The phases match perfectly between the annual and semiannual oscillations and the terannual oscillation. These three oscillations show larger amplitudes during solar maximum. The amplitude of the terannual oscillation is also correlated with the product of the amplitudes of annual and semiannual oscillations. According to the above features, it is suggested that the terannual oscillation might be related to the nonlinear interaction between the annual and semiannual oscillations[24].

3 Solar Cycle Variations of the Ionosphere

It is well known that the ionization effect of solar radiation principally forms the Earth's ionosphere. The intensity of solar EUV is found to fluctuate regularly and irregularly over timescales from minutes (flares), roughly 27 days (solar rotation) to decades (11-year solar cycle), with amplitudes varying up to more than 1000 times[25−26]. Accompanying the variations in solar activity, many parameters of the ionosphere/thermosphere fluctuate with similar periods and features[27−29]. Therefore, the solar activity effects on the ionosphere are essential and complicated.

Under the invitation from the editorial committee of Chinese Science Bulletin, Liu *et al.*[29] summarized some recent studies on solar activity effects of the ionosphere. Their short review reported some observations of solar irradiance at X-ray and EUV wavelengths and the outstanding problems of solar proxies in the view of ionospheric studies, new findings and improved representations of the features of the solar activity dependence of ionospheric key parameters and the corresponding physical processes, possible phenomena in the ionosphere under extremely high and low solar activity conditions, and statistical studies and model simulations of the ionospheric response to solar flares. In the following, some materials are taken from this review to keep the completeness of this national report. The reader is recommended to refer to Liu *et al.*[29] for details.

3.1 Solar Cycle Effects of the F_2 Peak

The F_2 peak is the most important region in the ionosphere, due to the highest electron density around the F_2 peak. Therefore, it has been the subject of most ionospheric investigations. Recent works studied some key parameters, such as f_0F_2 or N_mF_2[30−37], TEC[6−7,38−39], h_mF_2[31,34], plasma temperature and profile scale heights[31−40], thermospheric winds[41−43], and total mass density of the thermosphere[44]. These studies investigated the complicated responses of the ionosphere and thermosphere to changes in the solar activity, the related mechanisms, and how to represent those characteristics effectively in application missions[15,34−35].

The picture of solar activity effects of the ionosphere is gradually outlined in a more detailed way[30,32−33,46−47]. Many investigations have been conducted on the statistical relationship between ionospheric electron density and the solar proxy $F_{10.7}$. For example, Balan *et al.*[46], Liu *et al.*[32] and many others reported that the increase in TEC and N_mF_2 linearly follows the growth of $F_{10.7}$ under low and moderate solar activity levels, but the linearity breaks down at higher activity levels. Under such situations, TEC and N_mF_2 stop to increase and even turn to decrease at some stations.

It is under debate the nonlinear feature of the solar effects of the ionosphere and what causes such nonlinearities. Balan *et al.*[46−47] originally explained the saturation in electron density in response to the solar activity in terms of nonlinearity between solar indices and EUV intensity. Traditionally, the sunspot number R and $F_{10.7}$ are used for solar proxies.

However, Liu *et al.*[32] reported that the saturation effect is also detectable in f_0F_2 and EUV, and becomes stronger in equatorial anomaly regions. Liu *et al.*[34] further carried out an analysis based on a longest series of daily solar EUV data recorded by SOHO/SEM and N_mF_2 data recorded at global ionosonde stations in the East Asia/Australia sector. Their original objective was to quantify the solar activity sensitivity of daytime N_mF_2. Liu *et al.*[34] found that dynamic and chemical processes determine the seasonal and latitudinal features of the saturation effect. According to their results, the nonlinearity between solar EUV and $F_{10.7}$ is not enough to explain the observed saturation effect.

Kane[48] puzzled the inconsistency between the change rates in solar EUV intensity and those in N_mF_2. For example, solar EUV increased 150% from 1996 to 2000, while N_mF_2 changed from 210% to 290% at seven stations. Obviously, the solar EUV changes themselves were insufficient to account for

the observed changes in N_mF_2. It means that the solar activity not only determines the photoionization rates but also modulates various related processes. Liu *et al.*[34] reproduced the observed inconsistency of the change rates of solar EUV intensity and N_mF_2, if the solar activity effects of neutral compositions and chemical and dynamical processes are consistently taken into account. They further recommended an improved solar proxy $F_{10.7P}$ (here $F_{10.7P} = (F_{10.7}+F_{10.7A})/2$, $F_{10.7A}$ is the 81-day mean $F_{10.7}$), because $F_{10.7}$ and sunspot number fail to linearly represent the intensity of solar EUV.

Chen and Liu[49] further studied the influence of ionospheric dynamics and thermospheric variations on solar cycle effects of daytime N_mF_2. It is found that the variations of neutral atmosphere and h_mF_2, which is modulated by dynamic processes, are responsible for the seasonal and local time dependences of the linear increase rate of N_mF_2 on $F_{10.7}$ at mid-latitudes, while dynamic processes are the more important factors at low latitudes. Under high solar activities, dynamical processes not only control h_mF_2 to influence N_mF_2, but also directly slow down the change rate of N_mF_2 versus $F_{10.7}$, which is a key factor for causing the saturation effect.

A novel finding is that the solar activity effects of ionospheric electron density show linear, saturation and amplification features. The trends the ionosphere presented are found to be dependent on latitude, local time and season[5,30,39,50−51]. The solar activity variation in nighttime N_mF_2 at some stations retains the daytime saturation feature in summer, has a linear feature during the equinoxes, and presents an amplification feature in winter. Chen *et al.*[30] stated that dynamical processes (pre-sunset enhancement of the equatorial $\boldsymbol{E}\times\boldsymbol{B}$ vertical drift and neutral winds) and changes in neutral compositions contribute to the seasonal difference in the solar activity effects of nighttime N_mF_2. Liu and Chen[39] provided a quantitative description of the three kinds of solar activity effects in the global TEC. They illustrated the local time variation and longitudinal distribution of the TEC solar activity sensitivity in the four seasons. The saturation is found to cluster in equatorial anomaly regions, which were supported by Ma *et al*[52]. Ref. [52] used ionosonde N_mF_2 data to show latitudinal double peaks in the nonlinear coefficient of N_mF_2 versus solar proxies.

Recently, there are some attempts to search for usable ionospheric indices. Afraimovich *et al.*[6], She *et al.*[7] and Liu *et al.*[5] evaluated the mean TEC and its solar signature. These mean TEC data effectively depress the noise from local regions and capture obviously various time-scale variations in the solar activity[25,48,53], compared with individual TEC data. Moreover, the mean TEC averaged over latitude bands shows stronger solar activity sensitivity in lower latitude bands, and the saturation effect in the mean TEC versus $F_{10.7}$ is more pronounced at low latitudes, while the mean TEC increases more rapidly for higher solar EUV fluxes[5].

A long-lasting question in solar cycle effects of the ionosphere is the "hysteresis" phenomenon[38]. Similar to the "hysteresis" effect of magnetic materials, electron density may have different values for different phases of a solar cycle even at the same solar level. There is not yet an accepted explanation for the "hysteresis" effect. Attempts have been made in ionospheric models to include the possible influence of the historical state of the solar activity on the ionosphere[3,33]. The "hysteresis" effect, however, is difficult to reproduce effectively in nowadays models, which is one of the key problems restricting the development of long-term predictions of the ionosphere.

3.2 Solar Cycle Effects of the Ionosphere at Different Altitudes

To first order, the ionosphere varies with altitude. The solar cycle effect on ionospheric N_e profile and ion compositions is an interesting issue. Zhao *et al.*[18] studied the changes in topside ion compositions under different solar activities. Lighter ions (H^+ and He^+) dominate at 840 km altitude at LSA. With increasing solar activity, the main ions are gradually taken over by O^+. It means the upper transition

height, the altitude with equivalent number density of lighter ions and O^+, moves towards higher altitudes under high solar activities.

Under the assumption of diffusive equilibrium, the altitudinal distribution of the topside plasma density is determined by h_mF_2, N_mF_2 and plasma scale height. The plasma scale height naturally is an important parameter to describe the altitudinal distribution of plasma density in the topside ionosphere. In the light of this simplification, the peak parameters (h_mF_2, N_mF_2) and plasma scale height can be derived from the observations of incoherent scatter radar. Lei *et al.*[31] and Liu *et al.*[40] systematically investigated the climatology of plasma scale height around the F_2 layer peak, which are estimated from the observations of incoherent scatter radars at Arecibo (18.5° N, 66.8° W) and Millstone Hill (42.6°N, 288.5°E). The scale height linearly increases with $F_{10.7}$ and its variations have close relations with the thermal structure and dynamical processes in the ionosphere. They also discussed the possible connection between the scale height and N_e profile parameters, which has potential values in ionospheric models. Some parameters may be estimated from bottom-side profile parameters, providing the connection is strong enough.

Liu *et al.*[9,51] presented the climatology of plasma density at 840 km altitude. The data are the total ion density observed by DMSP. It is the first time to report that there are strong amplification features in the solar activity dependency of plasma density in the topside ionosphere. This feature becomes more obvious at lower magnetic latitudes. What is surprising to us is that the solar activity dependency of electron density becomes much complex, when the altitude moves downward to 600 km altitude[50]. ROCSAT-1 observations indicate that all the three patterns, linearity, saturation and amplification, can be found at 600 km altitude. In contrast, the saturation effect predominates at 400 km altitude[54]. Moreover, the equatorial anomaly feature is fairly obvious in the latitudinal distribution of ROCSAT-1 sunset plasma density, indicating the enhancement in equatorial vertical plasma drift during solar maximum.

According to the characteristics of ionospheric F-layer key parameters, Liu and Chen[17], Liu *et al.*[51] and Chen *et al.*[50] proposed an explanation to understand why there are three kinds of patterns at different altitudes in the solar activity response of the ionosphere. The principal factor controlling the solar activity variation trend of the plasma density at high altitudes (*e.g.*, 800 km) is the scale height, which drives the increase of the ionospheric plasma density in an exponential way. With the altitude moves downward, the scale height, h_mF_2 and N_mF_2 all play key roles. In particular, equatorial drift induces the change in h_mF_2, which further controls the solar activity response of the equatorial ionosphere.

3.3 Ionosphere Under Extreme Solar Conditions

The solar activity evolution itself is a very complicated and elusive process, and some extreme phenomena have been reported emerged in historical solar activities. For example, according to sunspot records on hand, virtually no sunspots were observed during the period of 1645−1715 (the Maunder Minimum), which indicates the Sun experienced an extremely long and low solar activity period.

Liu *et al.*[5] investigated the statistical relationship between ionospheric TEC and solar EUV. Negative values of plasma density are extrapolated, if one applies the statistical function of observed TEC and EUV to the situation that the Sun ceases to radiate EUV outward. The negative extrapolated TEC is certainly a non-physical result because the value of TEC should not be negative. However, it reveals a key point that under extreme solar conditions the state of the ionosphere should be different significantly from those under normal conditions. This gives rise to exploring how the ionosphere performs under such extremely low solar EUV radiation.

Smithtro and Sojka[55] conducted a pioneer work, in which they simulated the global average response of the ionosphere and thermosphere to different solar activities in terms of a global average

ionospheric/thermospheric model with assumptions of the solar EUV spectrum under extreme conditions. Their simulated results show that the change in neutral temperature and h_mF_2 with solar EUV intensity still keeps a linear rate even under extreme low solar conditions. With solar EUV decreasing to very low level, the molecular N_2 and O_2 are dense around the F_2 peak so that the electrons have a larger loss rate; as a consequence, the decrease in O^+ concentration is faster than that in molecular ions. Under such situations, the values of N_mF_2 become as low enough as those of N_mF_1, similar to the "G" condition in some storms. One feature we do not expect is that the simulated electron density grows faster when the solar activity goes beyond its normal range, which is consistent with that of the mean TEC observed in Liu *et al*[5].

It should be mentioned that the solar activity in 2007—2009 was low and extremely extended in recent solar minima. The spotless days reached 266 days in 2008, a record in 90 years. A campaign named "Deep Solar Minimum" is going on to investigate the response of the space environment to such unusual solar conditions. The behaviors of the ionosphere and thermosphere naturally become the hot spot in the international community of space physics.

Chen *et al*.[45] found that the ability of $F_{10.7}$ to indicate the intensity of solar EUV became worse during the period of 2007—2009. It means that the solar activity is surely unusual. Geomagnetic activity was much more quiet during the recent deep solar minimum than in the previous several solar minima (Fig. 2). A consequence of the calm geomagnetic activities is that the separation of atmospheric compositions accelerates, and the ratio of $[O]/[N_2]$ increases.

Solomon *et al*.[56] reported the total mass density of the upper atmosphere became smaller based on the atmospheric mass density database retrieved from the historical data of orbits of thousands of satellites. The total mass density normalized at 400 km altitude fell below 30% of those during previous solar minima, which means that the atmosphere became cooler.

Lühr and Xiong[57] compared the observed electron density from CHAMP and GRACE satellites with the predictions of an empirical ionospheric model[58] and showed that the prediction of the empirical model overestimates the ionospheric electron density in 2007—2009. In some sense, it also indicates the ionosphere behaviors were unusual during this period. Heelis *et al*.[59] also reported the ion temperature and the O^+/H^+ transition height became lower during this period.

Recently, Liu *et al*.[60] analyzed the global data of ionosondes and TEC GIMs during solar minima. Their results reveal a distinct decrease trend in N_mF_2 or f_0F_2, the virtual height of the F layer ($h'F$), and TEC during 2007—2009. The global mean TEC perfectly followed the reduction in solar EUV, reaching

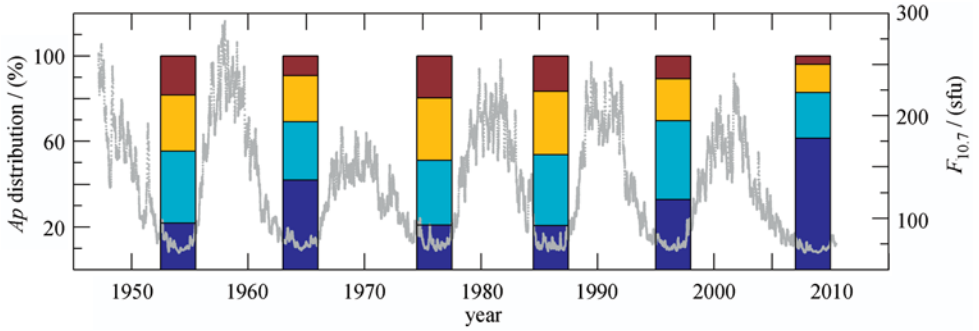

Fig. 2 Dot curve shows temporal series of $F_{10.7}$ during recent solar cycles, and bars show percentage distributions of Ap during solar minima ($F_{10.7} < 80$ sfu). Four segments, from top to bottom, of each bar for $Ap > 20$, $10 < Ap \leqslant 20$, $5 < Ap \leqslant 10$, and $Ap \leqslant 5$, respectively. After Chen *et al*.[45]

minimum in 2009. We can infer from the above studies that during the deep solar minimum the ionosphere responses in lower height and smaller electron density may be mainly attributed to the decrease in solar EUV.

As illustrated in Fig. 3, the 1-year running mean value of f_0F_2 drops 0.55 MHz at a Japanese station and the new proxy $F_{10.7\mathrm{P}}$ decreases about 3 sfu (solar flux unit). The work of Liu *et al.*[61] using COSMIC radio occultation measurements also supports this trend. Decrease in the intensity of solar EUV is proposed to act as the main driver for this decrease in ionospheric electron density. It deserves to stress that a quadratic fitting reasonably captures the solar variability of f_0F_2 and global average TEC at such low solar activity levels.

Araujo-Pradere *et al.*[62] also detected lower TEC over 4 middle latitude GPS stations in 2007—2009. It is interesting that they found a minor and marginal variation in ionosonde $N_\mathrm{m}F_2$. Therefore, different studies reported inconsistent changes in $N_\mathrm{m}F_2$ from solar minimum to minimum; which certainly calls for further investigation to gain a better understanding of the ionospheric behavior under such unusual solar conditions, to examine the data consistency, and to determine the influence of analysis techniques applied. It should be pointed out that Araujo-Pradere *et al.*'s analyses are based on the monthly median values in selected months, while others are 1-year running values. The conflict possibly reflects the different variability of the ionosphere over different timescales.

Unfortunately, we still lack the knowledge of solar EUV spectrum under extreme solar activity conditions from observations. Therefore, we have difficulty to preciously reproduce the picture of the ionosphere under such situations.

4 Ionospheric Empirical Modeling

Ionospheric sounding operated at Wuhan Ionospheric Observatory (WIO, 114.4° E, 30.6° N) has a history over 60 years, so WIO belongs to one of the stations with longest routine ionospheric observations. A series of single station models have been constructed on the basis of WIO observations. For example, Chen *et al.*[63] and Mao *et al.*[64] developed empirical models of TEC using the Fourier expansion and EOF repre-

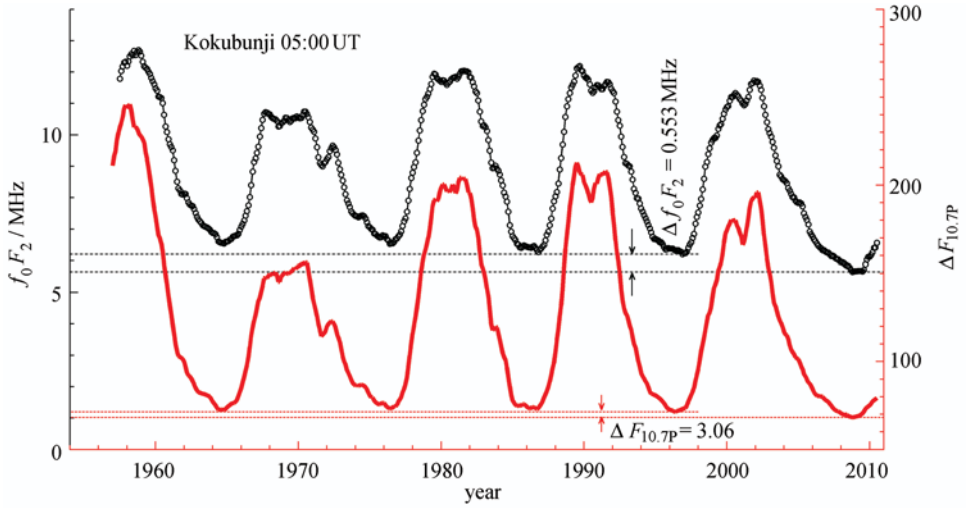

Fig. 3 Moving 1-year mean of f_0F_2 at Kokubunji (35.7° N, 139.5° E) at 05:00 UT (Universal Time) and $F_{10.7\mathrm{P}}$ over recent solar cycles. $F_{10.7\mathrm{P}} = (F_{10.7} + F_{10.7\mathrm{A}})/2$ in solar flux unit, 1 sfu = $10^{-22}\,\mathrm{W\cdot m^{-2}\cdot Hz^{-1}}$. Here, $F_{10.7\mathrm{A}}$ is the 81-day centered mean of $F_{10.7}$. The minimum value of f_0F_2 during solar minimum of cycle 23/24 is at least 0.553 MHz lower than those of the preceding cycles, and that of $F_{10.7\mathrm{P}}$ in cycle 23/24 is 3.06 sfu lower than those in the preceding cycles. After Liu *et al.*[60]

sentation methods, respectively. Liu *et al.*[33] built models of f_0F_2 using Fourier expansion and cubic-B splines approaches. The f_0F_2 models have good prediction accuracies with standard deviations in about 0.26 to 0.58 MHz. Yue *et al.*[65] gave a model regarding Wuhan f_0E. Liu *et al.*[66] adopted EOF method to develop a model of M(3000)F_2. In addition, through the work by Zhang and Huang[67], the bottom-side observations over Wuhan have been introduced in the International Reference Ionosphere (IRI), which has already improved the model description for the ionosphere in China.

Besides the data over Wuhan, Xu *et al.*[37] reconstructed a single station model using f_0F_2 data at Chongqing (29.4° N, 106.5° E).

Recently, Wan *et al.*[68] and E. A. *et al.*[69] conducted a complete EOF analysis of JPL-TEC and further constructed a TEC model. The global TEC model is constructed using the 1999−2009 GIMs provided by JPL. Their analyses also showed that EOF has outstanding advantage of fast convergence: the first four orders of the EOF series represent 99.04% of the overall variance of the original data set. Model-data comparisons indicate that the model can reflect the majority of the variations and the feature of temporal-spatial distribution of the global ionospheric TEC.

On the basis of the EOF base functions, Wan *et al.*[70] developed a now-casting system of TEC maps over China with real-time observation of TEC from four stations, Mohe, Beijing, Wuhan and Sanya, which distribute from the north to south of China.

In another work, E. A. *et al.*[71] discussed the impact of different model drivers through choosing appropriate proxies to present f_0F_2. They used similar-parameter interpolation method to optimally refill the missing points in original f_0F_2 series and applied an EOF analysis to construct empirical f_0F_2 models. The data are from three Japanese ionosonde stations, Wakkanai (45.4° N, 141.7° E), Kokubunji and Yamagawa (31.2° N, 130.6° E). The EOF analysis provided a set of base functions and associated coefficients. The diurnal variation of base functions reflects the essential nature of ionospheric f_0F_2, and the coefficients represent the variability. For example, the first order EOF coefficient reflects the solar cycle variation in the component.

Zhang and Holt[72] established an ionospheric electron temperature model based on incoherent scatter radar observations at Millstone Hill of America. Zhang *et al.*[73] built an ionospheric plasma temperature (ion and electron temperatures) model over French Saint Santin with a slightly higher geographic latitude but an lower apex latitude (14°) than Millstone. The French Saint Santin incoherent scatter radar observations covered over two solar cycles beginning in September 1965. Both mid-latitude ionospheric temperature models provide the climatological thermal status of the upper atmosphere. Comparisons with IRI predications indicate good agreement in ion temperature at high solar activity, and above the F_2 peak, while IRI electron temperature tends to be higher than both the St. Santin and Millstone Hill models.

Liu *et al.*[74] adopted the autocorrelation method to forecast the short-term variations in f_0F_2. They estimated the prediction errors to examine the forecast performances at Chongqing for different combinations of parameters and algorithms. Their work suggests the "at once" method for longer than 10 h predictions and the "iterations" method for shorter predictions. At the same time, the CRI model, a corrected method of IRI, was described. An effective ionospheric index was introduced into the CRI model to realize the regional forecasting in China region.

Yue *et al.*[75] made the first attempt to use an Artificial Neural Network (ANN) method to derive the possible long-term trend in f_0F_2. They analyzed f_0F_2 data at 19 ionospheric stations in the Asia/Pacific sector. A byproduct of their analysis is that the ANN method can effectively eliminate the geomagnetic activity effect on f_0F_2, compared to usual regression methods.

M(3000)F_2 is a key parameter to estimate h_mF_2.

Comparisons of empirical models with observations show a huge challenge for improving the presentation of M(3000)F_2. The CCIR option in IRI provides M(3000)F_2 with significant differences from observations, particularly in low latitude and equatorial regions.

Zhang *et al.*[76−77] made attempts to develop global models of M(3000)F_2 and h_mF_2. They also based on EOF methods to present the global climatology of the monthly median hourly values of ionosonde M(3000)F_2. The models were verified using data in 1965 (a low solar activity year) and 1970 (a high solar activity year). Better performance than IRI was showed by the comparisons between the model and observations.

The empirical presentation of the temporal and spatial variations of the ionosphere has vital values in applications. It is a long-lasting task. Here we wish to give some suggestions to future modeling for the ionosphere: (1) recommend $F_{10.7P}$[34] as solar proxy instead of $F_{10.7}$ and sunspot number; (2) adopt a quadratic approximation to describe the solar variability of electron density, instead of a linear fitting or other higher-order regression fittings; (3) include the equinoctial differences of the ionosphere; (4) effectively decrease the terms of the base functions in models with new analysis approaches (*e.g.*, EOF).

Acknowledgments This work was supported by the Chinese Academy of Sciences (KZZD-EW-01-3), National Key Basic Research Program of China (2012-CB825604) and National Natural Science Foundation of China (41074112, 41174137).

References

[1] Rishbeth H. How the thermospheric circulation affects the ionosphere F_2-layer [J]. *J. Atmos. Terr. Phys.*, 1998, **60**:1385-1402

[2] Yu T, Wan W, Liu L, Zhao B. Global scale annual and semi-annual variations of daytime N_mF_2 in high solar activity years [J]. *J. Atmos. Solar Terr. Phys.*, 2004, **66**:1691-1701

[3] Yu T, Wan W, Liu L, Tang W, Luan X, Yang G. Using IGS data to analysis the global TEC annual and semiannual variation [J]. *Chin. J. Geophys.*, 2006, **49**(4): 943-949

[4] Zhao B, Wan W, Liu L, *et al.* Features of annual and semiannual variations derived from the global ionospheric maps of total electron content [J]. *Ann. Geophys.*,2007, **25**(12):2513-2527

[5] Liu L, Wan W, Ning B, Zhang M L. Climatology of the mean TEC derived from GPS Global Ionospheric Maps [J]. *J. Geophys. Res.*, 2009, 114, A06308, doi:10.1029/2009JA014244

[6] Afraimovich E L, Astafyeva E I, Oinats A V, *et al.* Global electron content: a new conception to track solar activity. *Ann. Geophys.*, 2008, **26**:335-344

[7] She C, Wan W, Xu G. Climatological analysis and modeling of the ionospheric global electron content [J]. *Chin. Sci. Bull.*, 2008, **53**(2):282-288

[8] Zhao B, Wan W, Liu L, Yue X, Venkatraman S. Statistical characteristics of the total ion density in the topside ionosphere during the period 1996—2004 using Empirical Orthogonal Function (EOF) analysis [J]. *Ann. Geophys.*, 2005, **23**:3615-3631

[9] Liu L, Zhao B, Wan W, *et al.* Yearly variations of global plasma densities in the topside ionosphere at middle and low latitudes [J]. *J. Geophys. Res.*, 2007, 112, A07303, doi:10.1029/2007JA012283

[10] Li L Y, Jang J Y, Cao J B, *et al.* Statistical backgrounds of topside ionospheric electron density and temperature and their variations during geomagnetic activity [J]. *Chin. J. Geophys.*, 2011, **54**(10):2437-2444

[11] Liu L, Zhao B, Wan W, *et al.* Seasonal variations of the ionospheric electron densities retrieved from Constellation Observing System for Meteorology, Ionosphere, and Climate mission radio occultation measurements [J]. *J. Geophys. Res.*, 2009, 114, A02032, doi:10.1029/2008JA013819

[12] Zhang S R, Holt J M, Van Eyken A P, *et al.* IPY observations of ionospheric yearly variations from high- to middle-latitude incoherent scatter radars [J]. *J. Geophys. Res.*, 2010, 115, A03303, doi:10.1029/2009JA014327

[13] Balan N, Otsuka Y, Bailey G J, *et al.* Equinoctial asymmetries in the ionosphere and thermosphere observed by the MU radar [J]. *J. Geophys. Res.*, 1998, **103**:9481-9495

[14] Liu L, He M, Yue X, *et al.* The ionosphere around equinoxes during low solar activity [J]. *J. Geophys. Res.*, 2010, 115, A09307, doi:10.1029/ 2010JA015318

[15] Chen Y, Liu L, Wan W, Ren Z. Equinoctial asymmetry in solar activity variations of N_mF_2 and TEC [J]. *Ann. Geophys.*, 2012, **30**:613-622

[16] Ren Z, Wan W, Liu L, Chen Y, Le H. Equinoctial asymmetry of the ionospheric vertical plasma drifts and its effect on the F region plasma density [J]. *J. Geophys. Res.*, 2011, 116, A02308, doi:10.1029/2010JA016081

[17] Fuller-Rowell T J. The 'Thermospheric spoon': a mechanism for the semi-annual density variation [J]. *J. Geophys.*

Res., 1998, **103**:3951-3956

[18] Oliver W L, Kawamura S, Fukao S. The causes of the mid-latitude F layer behavior [J]. *J. Geophys. Res.*, 2008, 113, A08310, doi:10.1029/2007JA012590

[19] Ma R, Xu J, Liao H. The characteristics and a possible mechanism of semiannual variation of f_0F_2 [J]. *Chin. J. Geophys.*, 2002, **45**(6):766-772

[20] Ma R, Xu J, Liao H. The features and a possible mechanism of semiannual variation in the peak electron density of the low latitude F_2 layer [J]. *J. Atmos. Solar Terr. Phys.*, 2003, **65**:47-57

[21] Yu T, Wan W, Liu L, Lei J, Li X. Numerical study for the semi-annual variation of electric fields at the mid- and low-latitudes [J]. *Chin. J. Space Phys.*, 2006, **24**(3):182-193

[22] Zeng Z, Burns A, Wang W, *et al*. Ionospheric annual asymmetry observed by the COSMIC radio occultation measurements and simulated by the TIEGCM [J]. *J. Geophys. Res.*, 2008, 113, A07305, doi:10.1029/2007-JA012897

[23] Wan W, Xiong J, Ren Z, *et al*. Correlation between the ionospheric WN4 signature and the upper atmospheric DE3 tide [J]. *J. Geophys. Res.*, 2010, 115, A11303, doi:10.1029/2010JA015527

[24] Xu J, Ma R, Wang W. Terannual variation in the F_2 layer peak electron density (N_mF_2) at middle latitudes [J]. *J. Geophys. Res.*, 2012, 117, A01308, doi:10.1029/2011-JA017191

[25] Pap J, Bouwer S D, Tobiska W K. Periodicities of solar irradiance and solar activity indices [J]. *Solar Phys.*, 1990, **129**:165-189

[26] Lean J. Solar Ultraviolet irradiance variations: A review [J]. *J. Geophys. Res.*, 1987, **92**: 839-868

[27] Forbes J M, Bruinsma S, Lemoine F G. Solar rotation effects in the thermospheres of Mars and Earth [J]. *Science*, 2006, **312**:1366-1368

[28] Gorney D J. Solar cycle effects on the near-earth space environment [J]. *Rev. Geophys.*, 1990, **28**:315-336

[29] Liu L, Wan W, Chen Y, Le H. Solar activity effects of the ionosphere: A brief review [J]. *Chin. Sci. Bull.*, 2011, **56**(12):1202-1211

[30] Chen Y, Liu L, Le H. Solar activity variations of nighttime ionospheric peak electron density [J]. *J. Geophys. Res.*, 2008, 113, A11306, doi:10.1029/2008JA013114

[31] Lei J, Liu L, Wan W, Zhang S R. Variations of electron density based on long-term incoherent scatter radar and ionosonde measurements over Millstone Hill [J]. *Radio Sci.*, 2005, 40, RS2008, doi:10.1029/2004RS003106

[32] Liu J Y, Chen Y I, Lin J S. Statistical investigation of the saturation effect in the ionospheric foF2 versus sunspot, solar radio noise, and solar EUV radiation [J]. *J. Geophys. Res.*, 2003, **108**:1067

[33] Liu L, Wan W, Ning B. Statistical modeling of ionospheric f_0F_2 over Wuhan [J]. *Radio Sci.*, 2004, 39, RS2013, dio:10.1029/2003RS003005

[34] Liu L, Wan W, Ning B, *et al*. Solar activity variations of the ionospheric peak electron density [J]. *J Geophys. Res.*, 2006, 111, A08304, doi:10.1029/2006JA011598

[35] Richards P G. Seasonal and solar cycle variations of the ionospheric peak electron density: Comparison of measurement and models [J]. *J. Geophys. Res.*, 2001, **106**:12 803-12 819

[36] Sethi N K, Goel M K, Mahajan K K. Solar cycle variations of f_0F_2 from IGY to 1990 [J]. *Ann. Geophys.*, 2002, **20**:1677-1685

[37] Xu T, Wu Z S, Wu J, *et al*. Solar cycle variation of the monthly median f_0F_2 at Chongqing station China [J]. *Adv. Space Res.*, 2008, **42**:213-218

[38] Chakraborty S K, Hajra R. Solar control of ambient ionization of the ionosphere near the crest of the equatorial anomaly in the Indian zone [J]. *Ann. Geophys.*, 2008, **26**:47-57

[39] Liu L, Chen Y. Statistical analysis on the solar activity variations of the TEC derived at JPL from global GPS observations [J]. *J. Geophys. Res.*, 2009, 114, A10311, doi: 10.1029/2009JA014533

[40] Liu L, Le H, Wan W, *et al*. An analysis of the scale heights in the lower topside ionosphere based on the Arecibo incoherent scatter radar measurements [J]. *J. Geophys. Res.*, 2007, 112, A06307, doi:10.1029/2007JA012250

[41] Igi S, Oliver W L, Ogawa T. Solar cycle variations of the thermospheric meridional wind over Japan derived from measurements of f_mF_2. *J. Geophys. Res.*, 1999, **104**: 22 427-22 431

[42] Liu L, Wan W, Luan X, *et al*. Solar activity dependence of effective winds derived from ionospheric data at Wuhan [J]. *Adv. Space Res.*, 2003, **32**:1719-1924

[43] Liu L, Luan X, Wan W, *et al*. Solar activity variations of equivalent winds derived from global ionosonde data [J]. *J. Geophys. Res.*, 2004, 109, A12305, dio:10.1029/2004-JA010574

[44] Guo J, Wan W, Forbes J M, *et al*. Effects of solar variability on thermosphere density from CHAMP accelerometer data [J]. *J. Geophys. Res.*, 2007, 112, A10308, doi:10.1029/2007JA012409

[45] Chen Y, Liu L, Wan W. Does the $F_{10.7}$ index correctly describe solar EUV flux during the deep solar minimum of 2007—2009. *J. Geophys. Res.*, 2011, 116, A04304, doi:10.1029/2010JA016301

[46] Balan N, Bailey G J, Jenkins B, *et al*. Variations of ionospheric ionization and related solar fluxes during an intense solar cycle [J]. *J. Geophys. Res.*, 1994, **99**:2243-2253

[47] Balan N, Bailey G J, Moffett R J. Modeling studies of ionospheric variations during an intense solar cycle [J]. *J. Geophys. Res.*, 1994, **99**:17 467-17 475

[48] Kane R P. Solar EUV and ionospheric parameters: A brief

assessment [J]. *Adv. Space Res.*, 2003, **32**:1713-1718

[49] Chen Y, Liu L. Further study on the solar activity variation of daytime N_mF_2. *J. Geophys. Res.*, 2010, 115, A12337, doi:10.1029/2010JA015847

[50] Chen Y, Liu L, Wan W, *et al.* Solar activity dependence of the topside ionosphere in low latitudes [J]. *J. Geophys. Res.*, 2009, 114, A08306, doi:10.1029/2008JA013957

[51] Liu L, Wan W, Yue X, *et al.* The dependence of plasma density in the topside ionosphere on solar activity level [J]. *Ann. Geophys.*, 2007, **25**:1337-1343

[52] Ma R, Xu J, Wang W, Yuan W. Seasonal and latitudinal differences of the saturation effect between ionospheric N_mF_2 and solar activity indices [J]. *J. Geophys. Res.*, 2009, 114, A10303, doi:10.1029/2009JA014353

[53] Kane R P. Fluctuations in the 27-day sequences in the solar index F_10 during solar cycles 22—23 [J]. *J. Atmos. Solar Terr. Phys.*, 2003, **65**:1169-1174

[54] Liu H, Stolle C, Förster M, *et al.* Solar activity dependence of the electron density in the equatorial anomaly regions observed by CHAMP [J]. *J. Geophys. Res.*, 2007, 112, A11311, doi:10.1029/2007JA012616

[55] Smithtro C G, Sojka J J. Behavior of the ionosphere and thermosphere subject to extreme solar cycle conditions [J]. *J. Geophys. Res.*, 2005, 110, A08306, dio:10.1029/2004JA010782

[56] Solomon S C, Woods T N, Didkovsky L V, *et al.* Anomalously low solar extreme-ultraviolet irradiance and thermospheric density during solar minimum [J]. *Geophys. Res. Lett.*, 2010, 37, L16103, doi:10.1029/2010GL044468

[57] Lühr H, Xiong C. The IRI-2007 model overestimates electron density during the 23/24 solar minimum [J]. *Geophys. Res. Lett.*, 2010, 37, L23101, doi:10.1029/2010GL045430

[58] Bilitza D, Reinisch B W. International reference ionosphere 2007: Improvements and new parameters [J]. *Adv. Space. Res.*, 2007, **42**:599-609

[59] Heelis R A, Coley W R, Burrell A G, *et al.* Behavior of the O^+/H^+ transition height during the extreme solar minimum of 2008 [J]. *Geophys. Res. Lett.*, 2009, 36, L00C03, doi:10.1029/2009GL038652

[60] Liu L, Chen Y, Le H, Kurkin V I, Polekh N M, Lee C C. The ionosphere under extremely prolonged low solar activity [J]. *J. Geophys. Res.*, 2011, 116, A04320, doi:10.1029/2010JA016296

[61] Liu L, Le H, Chen Y, He M, Wan W, Yue X. Features of the middle and low latitude ionosphere during solar minimum as revealed from COSMIC radio occultation measurements [J]. *J. Geophys. Res.*, 2011, 116, A09307, doi:10.1029/2011JA016691

[62] Araujo-Pradere E A, Redmon R, Fedrizzi M, *et al.* Some characteristics of the ionospheric behavior during the solar cycle 23—24 minimum [J]. *Solar Phys.*, 2011, 270, doi:10.1007/s11207-011-9728-3

[63] Chen Y, Wan W, Liu L, Li L. A statistical TEC model based on the observation at Wuhan Ionospheric Observatory [J]. *Chin. J. Space Phys.*, 2002, **22**: 27-35 (in Chinese)

[64] Mao T, Wan W, Liu L. An EOF based empirical model of TEC over Wuhan [J]. *Chin. J. Geophys.*, 2005, **48**(4):751-758

[65] Yue X, Wan W, Liu L, Ning B. An empirical model of ionospheric f_0E over Wuhan [J]. *Earth Planets Space*, 2006, **58**:323-330

[66] Liu C, Zhang M L, Wan W, *et al.* Modeling $M(3000)F_2$ based on empirical orthogonal function analysis method [J]. *Radio Sci.*, 2008, 43, RS1003, doi:10.1029/2007RS003694

[67] Zhang S R, Huang X Y. Variations of bottomside electron density profile parameters obtained from observations at Wuchang, China [J]. *Adv. Space Res.*, 1998, **22**(6):749-752

[68] Wan W, Ding F, Ren Z, Zhang M L, Liu L, Ning B. Modeling the global ionospheric total electron content with empirical orthogonal function analysis [J]. *Sci. China Tech. Sci.*, 2012, 55, doi:10.1007/s11431-012-4823-8

[69] E A, Zhang D, Ridley A J, Xiao Z, Hao Y. A global model: Empirical orthogonal function analysis of total electron content 1999—2009 data [J]. *J. Geophys. Res.*, 2012, 117, A03328, doi:10.1029/2011JA017238

[70] Wan W, Ning B, Liu L, *et al.* Nowcasting the ionospheric total electron content over China [J]. *Prog. Geophys.*, 2007, **22**(4):1040-1045

[71] E A, Zhang D H, Xiao Z, Hao Y Q, Ridley A J, Moldwin M. Modeling ionospheric foF2 by using empirical orthogonal function analysis [J]. *Ann. Geophys.*, 2011, **29**:1501-1515

[72] Zhang S R, Holt J M. Ionospheric temperature variations during 1976—2001 over Millstone Hill [J]. *Adv. Space Res.*, 2004, **33**:963-969

[73] Zhang S R, Holt J M, Zalucha A M, Amory-Mazaudier C. Mid-latitude ionospheric plasma temperature climatology and empirical model based on Saint Santin incoherent scatter radar data from 1966—1987 [J]. *J. Geophys. Res.*, 2004, 109, A11311, doi:10.1029/2004JA010709

[74] Liu R, Xu Z, Wu J, Liu S, Zhang B, Wang G. Preliminary studies on ionospheric forecasting in China and its surrounding area [J]. *J. Atmos. Solar Terr. Phys.*, 2005, **67**:1129-1136

[75] Yue X, Wan W, Liu L, Ning B, Zhao B. Applying artificial neural network to derive long-term foF2 trends in the Asia/Pacific sector from ionosonde observations [J]. *J. Geophys. Res.*, 2006, 111, A10303, doi:10.1029/2005JA011577

[76] Zhang M-L, Liu C, Wan W, Liu L, Ning B. A global model of the ionospheric F_2 peak height based on EOF analysis [J]. *Ann. Geophys.*, 2009, **27**:3203-3212

[77] Zhang M L, Liu C, Wan W, Liu L, Ning B. Evaluation of global modeling of $M(3000)F_2$ and h_mF_2 based on alternative empirical orthogonal function expansions [J]. *Adv. Space Res.*, 2010, **46**:1024-1031